

Highly efficient p - i - n white organic light emitting devices with tandem structure

Meng-Huan Ho, Teng-Ming Chen, Pu-Cheng Yeh, Shiao-Wen Hwang, and Chin H. Chen

Citation: *Applied Physics Letters* **91**, 233507 (2007); doi: 10.1063/1.2822398

View online: <http://dx.doi.org/10.1063/1.2822398>

View Table of Contents: <http://scitation.aip.org/content/aip/journal/apl/91/23?ver=pdfcov>

Published by the *AIP Publishing*

Articles you may be interested in

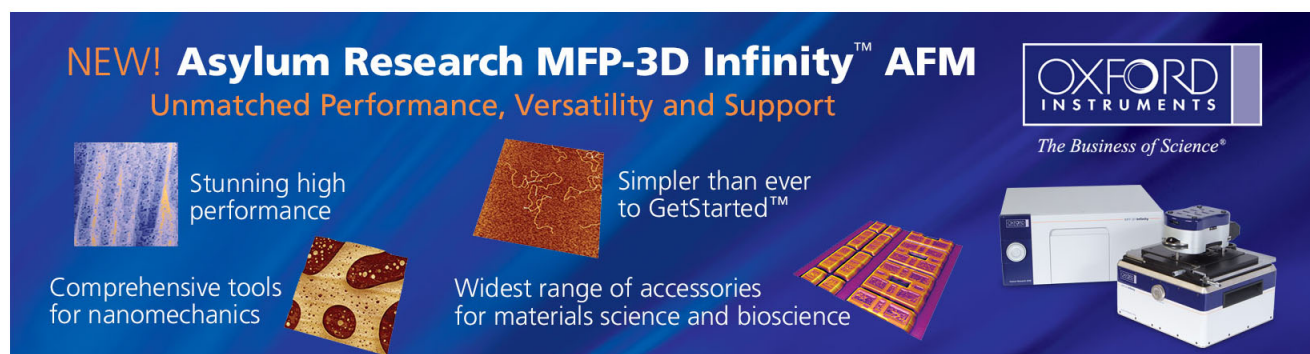
[Verification of p - n junctions in polymer light-emitting electrochemical cells via electrical characterization](#)
Appl. Phys. Lett. **95**, 101105 (2009); 10.1063/1.3224178

[Low voltage efficient simple p - i - n type electrophosphorescent green organic light-emitting devices](#)
Appl. Phys. Lett. **94**, 133303 (2009); 10.1063/1.3114378

[Solution processable ionic p - i - n phosphorescent organic light-emitting diodes](#)
Appl. Phys. Lett. **93**, 093302 (2008); 10.1063/1.2963032

[White p - i - n organic light-emitting devices with high power efficiency and stable color](#)
Appl. Phys. Lett. **91**, 113518 (2007); 10.1063/1.2784971

[High-efficiency and low-voltage p i n electrophosphorescent organic light-emitting diodes with double-emission layers](#)
Appl. Phys. Lett. **85**, 3911 (2004); 10.1063/1.1812378

The advertisement features a dark blue background with white and orange text. At the top left, it reads 'NEW! Asylum Research MFP-3D Infinity™ AFM' in large white letters, followed by 'Unmatched Performance, Versatility and Support' in orange. On the right, the Oxford Instruments logo is shown with the tagline 'The Business of Science®'. Below the text are four images: a textured surface, a circular pattern, a grid of small squares, and the AFM instrument itself. Each image is accompanied by a short text description: 'Stunning high performance', 'Simpler than ever to GetStarted™', 'Comprehensive tools for nanomechanics', and 'Widest range of accessories for materials science and bioscience'.

Highly efficient *p-i-n* white organic light emitting devices with tandem structure

Meng-Huan Ho^{a)} and Teng-Ming Chen

Department of Applied Chemistry, National Chiao Tung University, Hsinchu, Taiwan 300, Republic of China

Pu-Cheng Yeh

Department of Photonics and Institute of Electro-Optical Engineering, National Chiao Tung University, Hsinchu, Taiwan 300, Republic of China

Shiao-Wen Hwang and Chin H. Chen

Display Institute and Microelectronics and Information Systems Research Center, National Chiao Tung University, Hsinchu, Taiwan 300, Republic of China

(Received 6 September 2007; accepted 16 November 2007; published online 6 December 2007)

Highly efficient tandem *p-i-n* white organic light emitting devices have been fabricated. Utilizing an optical transparent bilayer with doped organic *p-n* junction that consists of 4,7-diphenyl-1,10-phenanthroline: 2% cesium carbonate (Cs_2CO_3)/*N,N'*-bis(1-naphthyl)-*N,N'*-diphenyl-1,1'-biphenyl-4,4'-diamine: 50% v/v tungsten oxide (WO_3) as the connecting layer, the tandem *p-i-n* white device achieved an electroluminescence efficiency of 23.9 cd/A and a power efficiency of 7.8 lm/W at 20 mA/cm² with a Commission Internationale de l'Eclairage coordinates of (0.30, 0.43). The electroluminescent color of this tandem *p-i-n* white organic light-emitting diode device will not change significantly with respect to drive current variation and forward viewing angle. © 2007 American Institute of Physics. [DOI: 10.1063/1.2822398]

Organic light-emitting diodes (OLEDs) are of considerable interest in recent years for flat panel display applications, particularly in white OLEDs (WOLEDs), which have attracted a lot of commercialization interests due to their demonstrated applications in the fabrication of full color displays with color filter¹ or as backlight for liquid crystal displays as well as in solid-state lighting.^{2,3} WOLEDs coupled with color filter for full color displays can circumvent the problematic issues of high resolution shadow mask and achieve higher effective aperture ratio of pixels.

For applications of WOLEDs, it is important that WOLEDs possess high brightness and electroluminescent (EL) efficiency at a lower current density and stable spectral characteristics in a wide range of injection current. By introducing a *p-i-n* structure to an OLED device, the operating voltage can be considerably reduced for both fluorescent⁴ and phosphorescent⁵ systems. The highly conductive *p*- and *n*-doped layers could enhance the charge injection from the contacts and reduce the Ohmic losses in these layers.⁴ Furthermore, many monochrome tandem OLEDs have been reported to be useful for providing high luminance.^{6,7} The luminance at a fixed current density increases linearly with the number of stacked and independent OLED elements. This can lead to a significant improvement in lifetime by reducing the degradation that accompanies the high drive currents required to achieve similarly high brightness in a single-unit device.

In this letter, we consolidate both the structural features of *p-i-n* technique and that of the tandem device concept into one WOLED device to modify the high drive voltage issue of reported tandem WOLEDs.^{8,9} The major challenge in tandem OLEDs in general is to prepare the effective connecting

layer between emitting units so that the current can smoothly flow through without facing substantial barriers. The organic doped bilayer in this study encompasses an *n*-doped organic layer and a *p*-doped organic layer to form a doped organic *p-n* junction at their contact interface, and offers several advantages, including excellent optical and electrical properties, as well as the ease of fabrication by thermal evaporation.

The architectures of the WOLED devices are shown in the inset of Fig. 1. Device I is the standard *p-i-n* WOLED unit with a dual emission layer (DEML) system,¹⁰ which gives rise to a balance white emission in thin thickness of 15 nm. The DEML system comprises one codopant emitting layer with 2-methyl-9,10-di(2-naphthyl)anthracene¹¹ (MADN): 5% *N,N'*-bis(1-naphthyl)-*N,N'*-diphenyl-1,1'-bi-

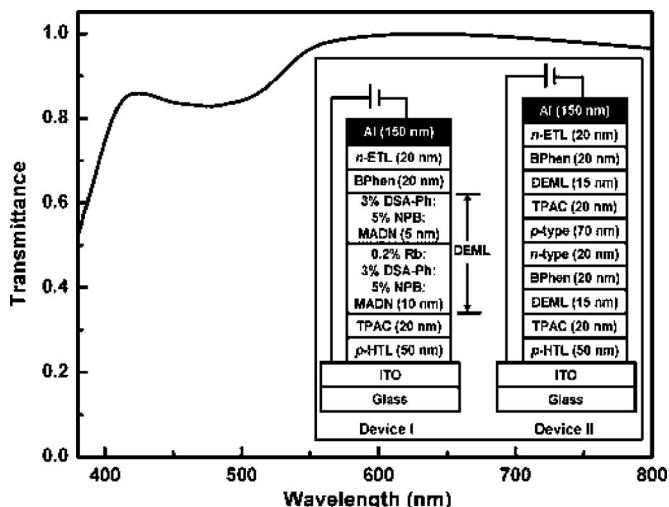


FIG. 1. Transmittance spectrum of BPhen: Cs_2CO_3 (20 nm)/NPB: WO_3 (70 nm) thin film. Inset: schematic device architecture of devices I and II.

^{a)} Author to whom correspondence should be addressed. Electronic mail: kinneas.ac94g@nctu.edu.tw

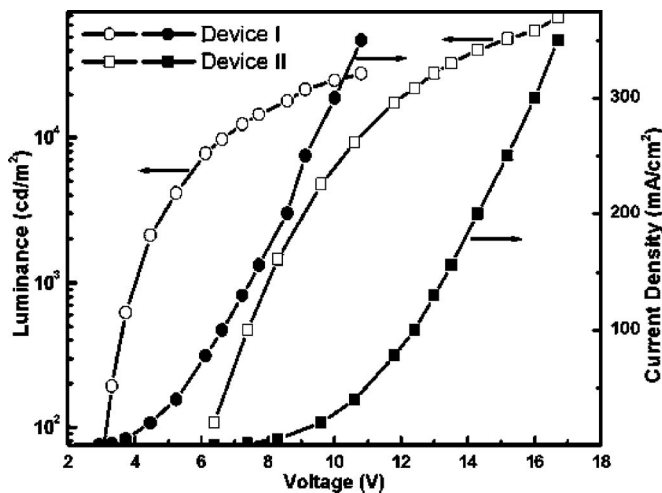


FIG. 2. Luminance-current density-voltage (L - J - V) characteristics of devices I and II.

phenyl-4,4'-diamine (NPB): 3% *p*-bis(*p*-*N,N*-diphenyl-aminostyryl)benzene¹¹ (DSA-Ph): 0.2% Rubrene (Rb) and one blue emitting layer of MADN: 5% NPB: 3% DSA-Ph. In the DEML system, MADN, NPB, DSA-Ph, and Rb were used as host material, assistant dopant, blue, and yellow fluorescent dopants, respectively. 1,1-bis[*N,N*-di(*p*-tolyl)aminophenyl]cyclohexane (TPAC)¹² and 4,7-diphenyl-1,10-phenanthroline (BPhen) were used as electron-blocker and hole-blocker materials to refine the exciton confinement. In our *p-i-n* architecture, 50% v/v tungsten oxide (WO₃) doped NPB (Ref. 13) and 2% cesium carbonate (Cs₂CO₃) doped BPhen (Ref. 14) were used as the *p*-doped transport layer and *n*-doped transport layer, respectively. Device II is the tandem *p-i-n* WOLED with stacking two WOLED units by a bilayer of organic doped thin film with optimized thickness consist of BPhen: 2% Cs₂CO₃/NPB (20 nm): 50% (v/v) WO₃ (70 nm). The *n*-type doped layer and the *p*-type doped layer are in contact with each other to form a doped organic *p-n* junction at their contact interface.

Figure 1 shows the transmittance of BPhen: 2% Cs₂CO₃ (20 nm)/NPB: 50% v/v WO₃ (70 nm) bilayer thin film and the connecting layer is transparent in the visible region from 420 to 750 nm, which is essential to achieve an efficient tandem WOLED. Figure 2 shows the L - V - J curves of devices I and II. Devices I and II achieved 2105 cd/m² and 4.5 V, 4780 cd/m², and 9.6 V at 20 mA/cm², respectively. As expected, the luminance and drive voltage increases with the increasing number of active units. Both devices I and II show near flat EL efficiency versus current density response as shown in Fig. 3. Device II with tandem structure achieved a current efficiency of 23.9 cd/A and an external quantum efficiency of 8.5% at 20 mA/cm², which is about 2.3 times greater than those of device I (10.5 cd/A and 3.9%). The enhanced EL efficiency is attributed to the effectiveness of the conductive *p-n* junction in electrically connecting two emitting units. Both light emissive units can efficiently produce light under the same current driving. It can also be observed that the power efficiency of device II (7.8 lm/W at 20 mA/cm²) is much higher than those of the reported fluorescent tandem WOLEDs (Refs. 9 and 10) due to the *p-i-n* structure of device II, which can effectively reduce the high drive voltage issue of tandem OLED device.

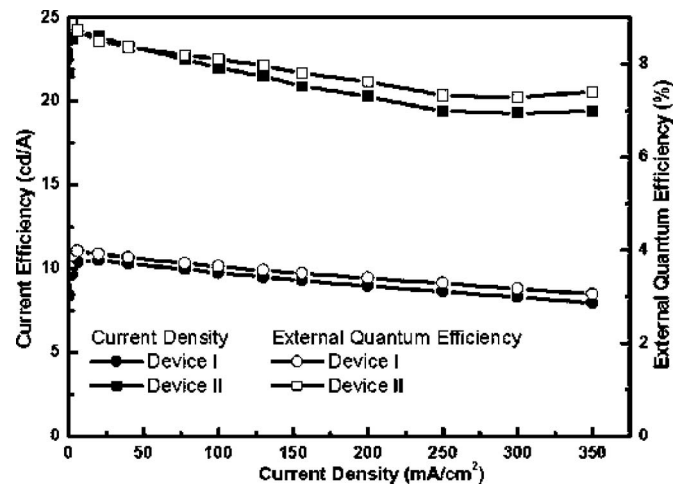


FIG. 3. Current efficiency and external quantum efficiency vs current density characteristics of devices I and II.

Figure 4 shows the EL spectra of devices I and II at 20 mA/cm² in the forward direction. The EL spectrum of device I covers a wide range of the visible region with three peaks at 470, 500, and 550 nm corresponding to the emissions from DSA-Ph (Ref. 11) and Rb, respectively, with CIE_{*x,y*} coordinates of (0.31, 0.42). The inset of Fig. 4 shows CIE_{*x,y*} coordinates versus luminance characteristics of device I and II. There is nearly no EL color shift of device I with respect to various luminance as the CIE_{*x,y*} coordinates only shift from (0.307, 0.416) at 2100 cd/m² to (0.295, 0.402) at 27800 cd/m² with Δ CIE_{*x,y*} of \pm (0.012, 0.014). This apparent resistance to color change under various drive current densities suggests the charge carriers for recombination are well-balanced in device I.¹⁰ With respect to device II, device II also simultaneously emits a balanced white color and an essentially identical EL spectrum with CIE_{*x,y*} coordinates of (0.30, 0.43) and no unexpected peak shift was observed, except the relative intensity of blue emission is slightly reduced and the full width of half maximum of device II (136 nm) is smaller than that of device I (144 nm). This phenomenon is not expected to result from shifting of the recombination zone because these devices were all driven at a fixed current. We attribute this slight spectrum change to the optical inter-

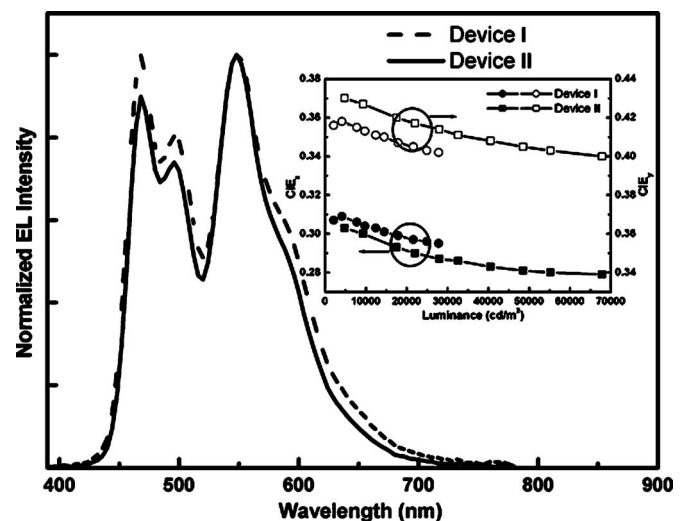


FIG. 4. EL spectra of devices I and II at 20 mA/cm². Inset: CIE_{*x,y*} coordinates vs current density characteristics of devices I and II.

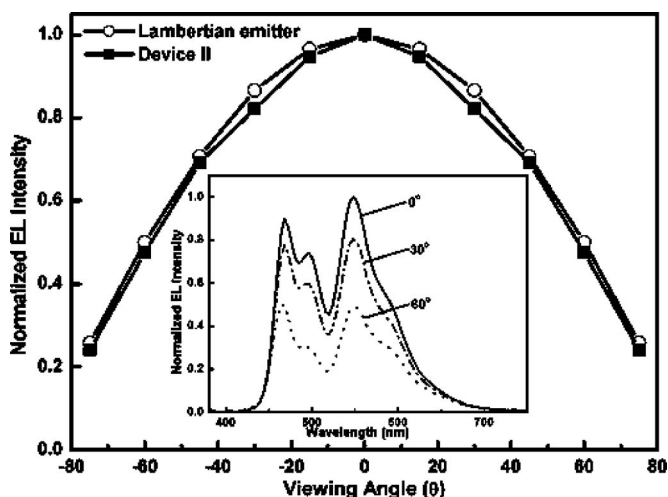


FIG. 5. Normalized EL intensity vs viewing angle characteristics of device II. Inset: EL spectra of device II under viewing angles of 0° , 30° , and 60° off the surface normal.

ference and minor microcavity effect in multilayer devices, which has been reported in tandem OLEDs.¹⁵ Under different levels of luminance, device II also reveals a stable EL color with $\Delta\text{CIE}_{x,y}$ of $\pm(0.024, 0.030)$ from $(0.303, 0.430)$ to $(0.279, 0.400)$ at a broad range from 4700 to 67800 cd/m^2 and nearly no current-induced quenching was observed either, as depicted in Fig. 3.

Another important factor of tandem WOLED devices is to obtain high EL efficiency and stable EL color with acceptable angular dependency characteristics. Figure 5 shows the normalized EL efficiency versus the viewing angle characteristics of tandem device II. It is generally assumed that the EL emission pattern from OLEDs is approximately Lambertian^{16,17} and it is clear that the angular dependence of device II is well fitted by a Lambertian distribution from Fig. 5. The EL spectra of device II under different viewing angles of 0° , 30° , and 60° were also shown in the inset of Fig. 5. It is noteworthy that the emission shows less angular dependence in device II as two main peaks of white emission at different viewing angles remain the same. The shifts in CIE x and y coordinates of device II from the viewing angle of 0° to 60° are only 0.024 and 0.01, respectively. In a strong microcavity effect, OLED devices potentially yield a non-Lambertian emission profile and cause a large angular-dependent color shift. According to our observation of the angular dependence of intensity and color, the microcavity

effect is minor in this tandem device which is in agreement with previous report.¹⁵

In summary, a tandem p - i - n WOLED device consists of two individual p - i - n WOLED units connected electrically with an optical transparent and doped organic p - n junction utilizing BPhen: Cs_2CO_3 /NPB: WO_3 have been fabricated. The charge-carriers for recombination of this tandem WOLED are well-balanced under various current densities due to the DEML system in each individual p - i - n WOLED, giving rise to one of the best EL efficiency of 23.9 cd/A and 7.8 lm/W with $\text{CIE}_{x,y}$ coordinates of $(0.30, 0.43)$. The electroluminescent color of this tandem p - i - n WOLED device will not change significantly with respect to drive current variation and forward viewing angle. This stratagem may provide an effective and promising way to achieve high-brightness WOLEDs.

This work was supported by a grant from Chunghua Picture Tubes, Ltd. (CPT) of Taoyuan, Taiwan. The authors also thank e-Ray Optoelectronics Technology Co., Ltd., of Taiwan for supplying some of the OLED materials studied in this work.

- ¹J. Kido, K. Nagai, and K. Okutama, Appl. Phys. Lett. **64**, 815 (1994).
- ²P. Destruel, P. Jolinat, R. Clergereaux, and J. Farenc, J. Appl. Phys. **85**, 397 (1999).
- ³B. W. D'Andrade and S. R. Forrest, Adv. Mater. (Weinheim, Ger.) **16**, 1585 (2004).
- ⁴J. Huang, M. Pfeiffer, A. Werner, J. Blochwitz, S. Liu, and K. Leo, Appl. Phys. Lett. **80**, 139 (2002).
- ⁵G. F. He, O. Schneider, D. S. Qin, X. Zhou, M. Pfeiffer, and K. Leo, J. Appl. Phys. **95**, 5773 (2004).
- ⁶L. S. Liao, K. P. Klubek, and C. W. Tang, Appl. Phys. Lett. **84**, 167 (2004).
- ⁷T. Y. Cho, C. L. Lin, and C. C. Wu, Appl. Phys. Lett. **88**, 111106 (2006).
- ⁸C. C. Chang, J. F. Chen, S. W. Hwang, and C. H. Chen, Appl. Phys. Lett. **87**, 253501 (2005).
- ⁹F. Guo and D. Ma, Appl. Phys. Lett. **87**, 173510 (2004).
- ¹⁰M. H. Ho, S. F. Hsu, J. W. Ma, S. W. Hwang, P. C. Yeh, and C. H. Chen, Appl. Phys. Lett. **81**, 113518 (2007).
- ¹¹M. T. Lee, H. H. Chen, C. H. Tsai, C. H. Liao, and C. H. Chen, Appl. Phys. Lett. **85**, 3301 (2004).
- ¹²P. M. Borsenberger, L. Pautmeier, R. Richert, and H. Bässler, J. Chem. Phys. **94**, 8276 (1991).
- ¹³C. C. Chang, M. T. Hsieh, J. F. Chen, S. W. Hwang, and C. H. Chen, Appl. Phys. Lett. **89**, 253504 (2006).
- ¹⁴S. Y. Chen, T. Y. Chu, J. F. Chen, C. Y. Su, and C. H. Chen, Appl. Phys. Lett. **89**, 053518 (2006).
- ¹⁵V. Bulovic, V. B. Khalifin, G. Gu, P. E. Burrows, D. Z. Garbuzov, and S. R. Forrest, Phys. Rev. B **58**, 3730 (1998).
- ¹⁶J. S. Kim, P. K. H. Ho, N. C. Greenham, and R. H. Friend, J. Appl. Phys. **88**, 1073 (2000).
- ¹⁷K. Saxena, D. S. Mehta, R. Srivastava, and M. N. Kamalasanan, Appl. Phys. Lett. **89**, 061124 (2006).